Hydride Shuttle Formation and Reaction with CO$_2$ on GaP(110)

Martina Lessio,[a] Thomas P. Senftle,[b, d] and Emily A. Carter*[c]

Adsorbed hydrogenated N-heterocycles have been proposed as co-catalysts in the mechanism of pyridine (Py)-catalyzed CO$_2$ reduction over semiconductor photoelectrodes. Initially, adsorbed dihydropyridine (DHP*) was hypothesized to catalyze CO$_2$ reduction through hydride and proton transfer. Formation of DHP* itself, by surface hydride transfer, indeed any hydride transfer away from the surface, was found to be kinetically hindered. Consequently, adsorbed deprotonated dihydropyridine (2-PyH$^-$*) was then proposed as a more likely catalytic intermediate because its formation, by transfer of a solvated proton and two electrons from the surface to adsorbed Py, is predicted to be thermodynamically favored on various semiconductor electrode surfaces active for CO$_2$ reduction, namely GaP(111), CdTe(111), and CuInS$_2$(112). Furthermore, this species was found to be a better hydride donor for CO$_2$ reduction than is DHP*. Density functional theory was used to investigate various aspects of 2-PyH$^-$* formation and its reaction with CO$_2$ on GaP(110), a surface found experimentally to be more active than GaP(111). 2-PyH$^-$* formation was established to also be thermodynamically viable on this surface under illumination. The full energetics of CO$_2$ reduction through hydride transfer from 2-PyH$^-$* were then investigated and compared to the analogous hydride transfer from DHP*. 2-PyH$^-$* was again found to be a better hydride donor for CO$_2$ reduction. Because of these positive results, full energetics of 2-PyH$^-$* formation were investigated and this process was found to be kinetically feasible on the illuminated GaP(110) surface. Overall, the results presented in this contribution support the hypothesis of 2-PyH$^-$*-catalyzed CO$_2$ reduction on p-GaP electrodes.

Introduction

World energy consumption continues to increase because of developing economies and a growing global population. At the same time, the increase in anthropogenic CO$_2$ emissions is causing severe changes to our climate that will deleteriously impact future generations. Renewable, clean energy sources are needed to address both of these issues. Photoelectrocatalytic CO$_2$ reduction to liquid fuels would provide a sustainable source of fuels that could reduce net atmospheric CO$_2$ emissions. Among the numerous systems for converting CO$_2$ into fuels or fuel precursors reported in the literature, a system developed by Bocarsly and co-workers appears especially promising.[1] In this system, CO$_2$ is reduced to methanol over a p-GaP

[a] Dr. M. Lessio
Department of Chemistry, Princeton University
Princeton, NJ 08544-1009 (USA)

[b] Dr. T. P. Senftle
Department of Mechanical and Aerospace Engineering
Princeton University, Princeton, NJ 08544-5263 (USA)

[c] Prof. E. A. Carter
School of Engineering and Applied Science
Princeton University, Princeton, NJ 08544-5263 (USA)
E-mail: eac@princeton.edu

[d] Dr. T. P. Senftle
Present address:
Department of Chemical and Biomolecular Engineering
Rice University, Houston, TX 77005 (USA)

Supporting Information and the ORCID identification number(s) for the author(s) of this article can be found under https://doi.org/10.1002/cssc.201800037.

photocathode under visible light irradiation and exposure to an acidified aqueous solution containing pyridine (Py). Methanol production was observed at nearly 100% faradaic efficiency and at underpotentials more than 300 mV below the thermodynamic potential associated with this CO$_2$ reduction process. Although p-GaP photocathodes have exhibited the best performance to date, intriguing observations on other electrode materials (Pd,[2] Pt,[3] CdTe,[4] and CuInS$_2$[5,6]) exposed to acidified aqueous solutions containing Py confirm that this aromatic amine is a required ingredient in the catalytic mechanism. Understanding the catalytic role played by Py is an essential step towards the development of an efficient technology for converting CO$_2$ into liquid fuels by using solar energy.

Numerous experimental and computational studies have been conducted by different research groups to shed light on the catalytic mechanism. Here, we present a brief overview of these investigations, focusing on the results that provide motivation for the research presented herein. Our group proposed the first mechanism specific to Py-catalyzed CO$_2$ reduction on p-GaP photoelectrodes.[7–9] This mechanism involves adsorbed dihydropyridine (DHP*) as the active catalyst, which reduces CO$_2$ to HCOOH by transferring a hydride and a proton. DHP* is proposed to form by the reaction of adsorbed pyridine (Py*) with a surface hydride (H$^-$*) and a proton from solution. In a more recent study,[10] our group proposed that the precursors needed for DHP* formation might be generated by a one-electron reduction of pyridinium (PyH$^+$) to Py* and an adsorbed hydrogen atom (H*). H$^-$* may then form through H* reduction

by a second electron from the surface. PyH$^+$ is present in significant concentration in solution, given that its pK_a of 5.2 is nearly equal to the aqueous solution's pH of 5.3, in the experimental system of Bocarsly and co-workers.[1] Alternatively, Py* might form simply through Py adsorption from solution, based on previous adsorption free energy predictions and experiments showing that Py favorably adsorbs on this surface,[11–13] and H$^-$* might form by dissociative adsorption of water and reduction by GaP surface electrons. In fact, a previous combined experimental–computational study of the GaP(110) surface exposed to water showed that partial water dissociation is thermodynamically favored on this surface at room temperature, which yields adsorbed protons that develop hydride character.[14, 15] Furthermore, in a separate study we demonstrated that adsorbed protons generated by heterolytic water dissociation on the GaP(110) surface are highly stable and thus can be further reduced to H$^-$*.[13] These studies and other previous ones by our group[8–11, 13, 14, 16, 17] focused on the GaP(110) surface, because it is the most thermodynamically stable surface of GaP.[18]

The heterogeneous mechanism for DHP*-catalyzed CO$_2$ reduction on p-GaP photoelectrodes proposed by our group is consistent with several experimental and theoretical findings. First, it has been observed that the selectivity of the CO$_2$ reduction process, as well as the applied potential required for the process to occur, depends on the electrode material,[1–6] thus supporting the hypothesis of a heterogeneous mechanism. Such a hypothesis is supported further both by recent predictions from our group[16] and measurements by the Bocarsly group.[19] Bocarsly and co-workers observed that the GaP(110) surface is more active towards CO$_2$ reduction than the GaP(111) surface.[19] If the CO$_2$ reduction mechanism in this system were homogeneous, then this observation could be explained only by a substantial difference in the energy of the photoexcited electrons provided by the two surfaces. However, we found that the conduction band minima (CB$_{min}$) of the two surfaces lie very close, with a difference of less than 0.1 V.[16] Therefore, we concluded that a homogeneous mechanism cannot explain these experimental observations, and that the mechanism must involve adsorbed intermediates. Several adsorption free energy studies found that Py and DHP favorably bind to the GaP surface, whereas CO$_2$ does not.[11–13] These results support the hypothesis of DHP* formation by Py* reduction and the need for an adsorbed co-catalyst (e.g., DHP*) to shuttle electrons from the surface to CO$_2$. The hypothesis of Py* reduction to DHP* is also supported by the moderate value of the computed reduction potential for this process to occur (-0.71 V vs. the saturated calomel electrode, SCE),[8, 9] which lies well below the GaP CB$_{min}$ (-1.76 V vs. SCE computed for the solvated GaP(110) surface and -1.68 V vs. SCE computed for the solvated reconstructed GaP(111) surface).[16]

The hypothesis that the precursors needed for the adsorbed catalyst formation are generated via PyH$^+$ reduction[10] is consistent with the experimental observation that an acidic pH is an essential condition for CO$_2$ reduction to occur.[2] The computed reduction potential for PyH$^+$ reduction to Py* and H* (-0.85 V vs. SCE)[10] again lies well below the GaP CB$_{min}$, thus

suggesting that the process is thermodynamically feasible on p-GaP photocathodes under illumination. The hypothesis of a DHP-based co-catalyst is further supported by recent experimental work, albeit on a metal rather than semiconductor surface. In a study using Pt electrodes, PyH$^+$ was observed to undergo hydrogenation through transfer of surface hydrogen atoms under electrochemical conditions similar to the ones applied in the CO$_2$ reduction experiments.[20] In a different study using Pt and glassy carbon electrodes under applied negative bias, CO$_2$ reduction to formic acid and methanol was observed in the presence of a DHP-like species.[21] These studies suggest that hydrogenated N-heterocycles (HNHs) can form on electrode surfaces under electrochemical conditions, and that such HNHs might be responsible for the heterogeneous reduction of CO$_2$.

Alternative mechanisms for Py-catalyzed CO$_2$ reduction have been proposed by other groups. Musgrave, Hynes, and co-workers proposed a homogeneous mechanism in which the active catalyst is solvated DHP, formed from a 1-pyridinyl radical (1-PyH$^·$) intermediate.[22] They proposed that this radical is generated by a one-electron reduction of PyH$^+$ in solution and that photoexcited electrons from the p-GaP photoelectrode have enough energy to promote this process. In a recent study,[16] we confirmed that GaP(110) CB$_{min}$ has a more negative reduction potential than PyH$^+$ + e$^-$ → 1-PyH$^·$ (-1.44 V,[23] -1.44 V,[24] -1.31 V,[25] and -1.58 V[26] vs. SCE). However, these two levels lie very close and, especially when considering the uncertainty of these computed values, we concluded that the process is likely kinetically hindered.[16] In addition, the alternative pathway for PyH$^+$ reduction introduced above (PyH$^+$ + e$^-$ → Py* + H*) has a much lower reduction potential, thus suggesting that PyH$^+$ + e$^-$ → 1-PyH$^·$ is unlikely to compete with it. Finally, the Musgrave–Hynes mechanism is entirely homogeneous, which is inconsistent with our recent findings[16] combined with the experimental observations by Bocarsly and co-workers[19] showing that adsorbed intermediates must be involved in the CO$_2$ reduction mechanism. A heterogeneous mechanism specific for Pt electrodes was proposed by Batista and co-workers.[26] The reduction potentials and activation free energies ($\Delta G^{\ddagger}$) calculated for this mechanism suggest that it is energetically feasible under experimental conditions. However, the only role of PyH$^+$ in this mechanism is to act as a proton source, which is not specific enough to explain the catalytic effect of Py observed in the experimental studies discussed above.

Based on mounting evidence supporting the hypothesis of DHP*-catalyzed CO$_2$ reduction, we recently went on to investigate the energetics of DHP* formation[17] via the mechanism previously proposed (i.e., H$^-$* transfer and proton transfer from solution to Py*).[8, 9] We found that this mechanism, although thermodynamically favored, is likely kinetically hindered, as H$^-$* transfer away from the surface is unfavorable.[17] We therefore concluded either that there is a more kinetically favorable pathway for DHP* formation or that a different Py-derived HNH forms and is responsible for catalyzing CO$_2$ reduction. In that study, we used our computed thermodynamic hydricities to demonstrate that DHP*, if formed, would be a capa-

ble hydride donor for reducing CO_2. However, we also discovered that, not surprisingly, adsorbed deprotonated 1,2-(*ortho*)-dihydropyridine (2-PyH$^-$*) would be a much better hydride donor for CO_2. In a separate study, we also found that the formation of 2-PyH$^-$* through transfer of photoexcited electrons and a proton from solution is thermodynamically feasible on reconstructed GaP(111), CdTe(111), and CuInS$_2$(112) surfaces under illumination.[27]

The complete mechanism proposed for 2-PyH$^-$* formation and reaction with CO_2 resulting in HCOOH formation is depicted in Scheme 1. In this mechanism, 2-PyH$^-$* is formed either
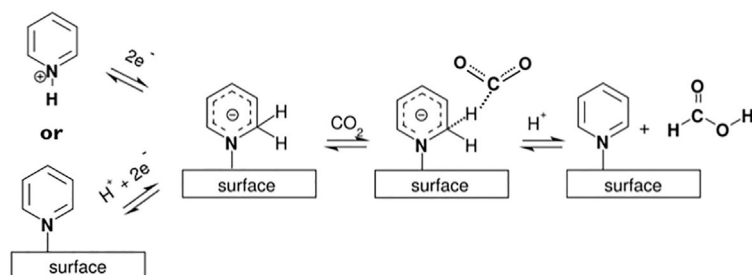
Scheme 1. Proposed mechanism of adsorbed deprotonated dihydropyridine (2-PyH$^-$*) formation and reaction with CO_2. 2-PyH$^-$* formation can occur either by two-electron reduction of solvated pyridinium (PyH$^+$) or by proton-coupled two-electron transfer to adsorbed pyridine (Py*).

by a two-electron reduction and isomerization of PyH$^+$ or by a proton-coupled two-electron transfer (PC2ET) to Py*. 2-PyH$^-$* then transfers a hydride to CO_2, forming either HCOO$^-$ or HCOOH depending on the pH at the interface. Although the detection of formate/formic acid intermediates has only been reported for Pt[3] and CdTe[4] electrodes in the presence of Py, we can expect the mechanism on p-GaP electrodes to proceed through a similar initial step that generates such intermediates.

In this study, we use cluster model and periodic boundary condition (PBC) calculations with density functional theory (DFT)[28] to investigate various aspects of the proposed mechanism shown in Scheme 1 for the GaP(110) surface. We also compare these results to previous ones obtained for the reconstructed GaP(111) surface to further understand the observed difference in activity between the two surfaces.[19] We first verify that 2-PyH$^-$ favorably adsorbs on the GaP(110) surface and thus can play the role of adsorbed co-catalyst. We then compare the predicted reduction potentials associated with 2-PyH$^-$* formation to the GaP(110) CB$_{min}$ to establish whether these reactions are feasible given the energy of photoexcited electrons originating from this surface. We also compare the computed reduction potential to the reduction potentials for other previously proposed reactions that might compete with 2-PyH$^-$* formation. We then compare the predicted reaction energetics for hydride transfer from 2-PyH$^-$* to CO_2 and hydride transfer from DHP* to CO_2 to verify that 2-PyH$^-$* is indeed a better hydride donor, as suggested by the thermodynamic hydricities computed in our previous study.[17] We conclude our study by investigating the kinetics of 2-PyH$^-$* forma-

tion on the GaP(110) surface to establish whether this newly proposed catalytic intermediate can be formed under experimental conditions.

Theoretical Methods

We employ solvated cluster models to compute adsorption free energies, reduction potentials, and reaction energetics for selected reactions occurring on the electrode surface. All calculations were performed with the computational chemistry software Orca (version 3.0.3),[29] using DFT with the B3LYP[30–32] exchange-correlation (XC) functional. Ga atoms were represented by a Stuttgart effective core potential (ECP28MWB, with the MWB core potential simulating the nucleus and the inner 28 electrons) and the associated double-zeta valence basis set simulating the three remaining valence electrons[33,34] to carry out both geometry optimizations and single-point energy calculations. For all of the other atoms, we used all-electron Pople 6-31G** basis sets[35,36] to carry out geometry optimizations and aug-cc-pVDZ basis sets[37] to carry out subsequent single-point energy calculations. Grimme's D2 dispersion correction[38] was applied in all calculations to better account for adsorbate–surface interactions. The accuracy of this computational method, together with the cluster model, was validated previously against benchmark periodic slab calculations performed with a converged planewave basis set.[11] We used the same mixed implicit–explicit solvation approach employed in previous work[13,17] to improve the description of solvation effects when calculating adsorption free energies, reduction potentials, and reaction energetics. This approach consists of using the implicit solvation model based on solute electron density (SMD)[39] in the presence of a full monolayer of half-dissociated water molecules adsorbed on the cluster surface. This water configuration was found to be the most thermodynamically stable one in our previous combined computational–experimental characterization of the GaP(110)/water interface.[14,15] We refer the reader to our previous reports[13,17] for further details and justification for this solvation approach choice.

We used the same GaP(110) cluster model employed in previous studies[10,11,13,16,17] and built following the procedure reported in ref. [11]. The cluster structure includes 24 Ga atoms, 24 P atoms, and 40 H atoms. The H atoms saturate the dangling bonds formed at the bottom and side cluster surfaces after carving the cluster out from the periodic surface model. The top surface of the cluster model does not have dangling bonds and thus can be used to simulate adsorption phenomena and surface reactions. More details and figures of the cluster model are provided in our previous reports cited above (see, for instance, the Supporting Information of ref. [13]).

Adsorption free energies were computed with the equation given in the Supporting Information. We followed the same procedure described in our previous report[13] to generate the free adsorption sites needed to simulate species adsorption on the explicitly solvated cluster surface. Reduction potentials

were calculated from reaction free energies (ΔGs) in solution using the method summarized in the Supporting Information and thoroughly discussed in ref. [10]. As discussed there, we used the value of $-104.3 \, \text{kcal mol}^{-1}$ for the free energy of a solvated electron, which is derived from the absolute potential of the standard hydrogen electrode (SHE, $-4.281 \, \text{V}$)[40] shifted by $-0.244 \, \text{V}$ to report our reduction potentials on the SCE scale. The free energy of a proton in solution was set to $-270.3 \, \text{kcal mol}^{-1}$, which is an empirical value derived from different contributions thoroughly described in ref. [41]. ΔG and $\Delta G^{\ddagger}$ values were computed by using the "supermolecule approach", in which all species, including those that are not directly adsorbing on the cluster surface (e.g., CO_2), are simulated in the same calculation in contact with each other. In our previous study, we also tested a "separate reactant approach" (in which the free energy of each reactant species is calculated in a separate calculation) and found reasonably similar results.[17]

We performed frequency calculations to verify local minima and transition states. A true minimum exhibits no imaginary frequencies, whereas a transition state must possess only one imaginary frequency corresponding to the correct reaction coordinate. To verify that the transition state found is actually the relevant one, we structurally relaxed each transition-state structure by following the vibrational mode associated with the imaginary frequency along both steepest descent directions and checked that the expected initial and final states for the reaction under study were reached. Transition-state optimizations were carried out by using the eigenvector-following method available in Orca.[42] The vibrational frequencies were used also to calculate thermal corrections at room temperature (298.15 K), which were computed using the ideal gas, rigid rotor, and harmonic oscillator approximations. Note that translational and rotational contributions are zero for calculations involving the cluster model, as it is used to simulate an extended crystal surface with only vibrational degrees of freedom.

PBC calculations were used to study the energetics of 2-PyH$^-$* formation at the GaP(110) surface. These calculations were carried out using the Vienna Ab initio Simulation Package (VASP)[43–45] and DFT with the PBE XC functional.[46] We used the projector-augmented-wave (PAW) method[47] and the default PAW potentials available in VASP[48] to simulate all nuclei (Ga, P, N, C, O, and H) and frozen core electrons ($1s \, 2s \, 2p \, 3s \, 3p \, 3d$ for Ga, $1s \, 2s \, 2p$ for P, $1s$ for N, $1s$ for C, and $1s$ for O). We simulated the remaining electrons by using a plane-wave basis with an 800 eV kinetic energy cutoff. We sampled the Brillouin zone with a $2 \times 2 \times 1$ k-point mesh based on the Monkhorst–Pack Scheme.[49] We integrated the Brillouin zone using the Gaussian smearing method with a smearing width equal to 0.05 eV. These computational settings allowed us to reach a convergence on the total energy to within 1 meV per atom. Grimme's D2 dispersion correction[38] was also applied in this type of calculation.

We used the same slab model for the GaP(110) validated in our previous report[11] and already employed in other previous studies.[10,16] This model consists of a 2×3 supercell with a five-layer thickness. We kept the atoms of the central layer frozen

in their bulk positions during geometry optimization to simulate a semi-infinite crystal. The vacuum region in between the two surfaces of the slab was larger than 20 Å to avoid interaction between periodic images along the direction perpendicular to the slab surface. In our previous studies, we placed adsorbates on both sides of the slab to prevent the development of artificial dipoles.[10,12,14–16] In this work, we used the climbing-image nudged-elastic-band (CI-NEB) method[50] to identify transition-state structures (see below), which we were not able to converge with mirrored adsorbates. Therefore, we instead only adsorbed species on one side of the slab and applied dipole corrections as implemented in VASP. We performed vibrational frequency analyses to verify energy minima and transition states, as well as to compute thermal corrections. Given the large size of the unit cell (157 atoms), we included only the adsorbate atoms in the vibrational frequency analysis and neglected contributions from surface Ga and P atoms. This is a valid approximation, given that our goal is to compute free energy differences (i.e., ΔG and $\Delta G^{\ddagger}$ values), and the contributions from the Ga and P slab atoms are likely to be very similar for reactant-, transition-, and final-state structures because they do not undergo major displacements during the reaction. We calculated frequencies by using a numerical Hessian constructed from finite differences of analytic gradients and ± 0.02 Å displacements.

Transition-state structures were identified by using the CI-NEB procedure developed by Henkelman et al.[50] These calculations employed a 600 eV planewave basis kinetic energy cutoff for computational efficiency during the CI-NEB search; thereafter the energy of the final transition state was refined with a single-point calculation at 800 eV to be consistent with the kinetic energy cutoff used to identify the reactant and product endpoint geometries used in the CI-NEB search. The reaction coordinate was populated with four evenly spaced images (interpolated structures) along the reaction coordinate, where tangential forces on each image were minimized below $0.05 \, \text{eV Å}^{-1}$ along the minimum energy path. The transition-state structure was confirmed with a frequency analysis, which exhibited a predominant imaginary frequency ($1341.3 \, i \, \text{cm}^{-1}$) along the PC2ET coordinate. Multiple imaginary frequencies below $100 \, i \, \text{cm}^{-1}$ were also present and could not be removed despite numerous attempts to refine the transition-state structure. These frequencies are associated with rotations of H_2O molecules in the explicit solvation layer and are not involved in the PC2ET reaction coordinate (Table S1 in the Supporting Information).

Results and Discussion

Adsorption of deprotonated dihydropyridine on GaP(110)

The first step towards assessing the feasibility of the proposed mechanism in Scheme 1 is to evaluate the adsorption free energy of 2-PyH$^-$ on GaP(110) at room temperature, to determine whether it can play the role of an adsorbed catalytic intermediate. 2-PyH$^-$ is adsorbed in an analogous way to the previously proposed catalytic intermediate DHP (i.e., via a

dative bond from N to a surface Ga). The adsorption free energies were computed by using both implicit solvation only and our mixed implicit–explicit solvation approach (as done in our previous study[13]) to test the effect of water co-adsorption on the stability of adsorbed intermediates. We find that 2-PyH⁻ is favorably adsorbed on the GaP(110) surface with an adsorption free energy of −32.7 kcal mol⁻¹ computed with our mixed implicit–explicit approach. The adsorption free energy computed with implicit solvation only is significantly lower (−24.7 kcal mol⁻¹). Including the explicit layer of adsorbed water molecules has a large stabilization effect due to the hydrogen bond formed between one of the two 2-PyH⁻ N lone pairs and a co-adsorbed water molecule. The adsorption free energy of 2-PyH⁻ is also significantly more negative than the adsorption free energy of previously studied Py-related intermediates (−9.3 kcal mol⁻¹ for Py,[10] −8.2 kcal mol⁻¹ for 1,2-(ortho)-dihydropyridine (o-DHP),[10] and −12.9 kcal mol⁻¹ for 2-PyH˙,[16] computed with implicit solvation only). This larger binding energy probably originates from the negatively charged 2-PyH⁻ having a larger driving force to form a strong dative bond with a surface Ga atom, which carries a partial positive charge. Overall, these results suggest that 2-PyH⁻ is a promising candidate for the relevant adsorbed catalytic intermediate on the GaP(110) surface, in agreement with previous investigations over the reconstructed GaP(111), CdTe(111), and CuInS₂(112) surfaces.[27]

Formation thermodynamics of adsorbed deprotonated dihydropyridine on GaP(110)

Next, we determine whether formation of 2-PyH⁻* on GaP(110) is thermodynamically feasible under experimental conditions by computing reduction potentials associated with its hypothesized formation paths from solvated PyH⁺ and adsorbed Py (Scheme 1). We also compare these reduction potentials to those associated with reducing adsorbed Py to adsorbed o-DHP or 2-PyH˙, along with those associated with various PyH⁺ reduction pathways previously proposed in other studies (Table 1). Note that we only consider one of the two possible isomers of DHP: o-DHP. This choice was already justified in previous reports.[10,13,17]

We can determine whether 2-PyH⁻* formation on GaP(110) is feasible under experimental conditions by comparing the computed reduction potentials associated with its formation (Table 1) to the CB_min of solvated GaP(110) computed in our previous study (−1.66 V vs. SCE at pH 5.2).[16] The reduction potentials reported in Table 1 were computed with and without explicit solvation of the cluster surface (results obtained without explicit solvation are reported in parentheses). Unlike most other reductions in Table 1, including explicit water molecules on the cluster surface significantly affects the reduction potentials for formation of 2-PyH⁻*, which become less negative. The origin of these shifts is the stabilization provided by the hydrogen bond formed between an explicit water molecule and the negatively charged N atom belonging to 2-PyH⁻*. This physical effect should not be neglected; we therefore focus on the mixed implicit–explicit solvation predictions here. Accordingly, we see that both 2-PyH⁻* formation paths have reduction potentials less negative than the GaP(110) CB_min (−1.09 V and −0.86 V vs. SCE for formation via adsorbed Py reduction and PyH⁺ reduction, respectively). Although both pathways are thermodynamically viable, formation by PyH⁺ reduction is the least endoergic and thus could be the preferred pathway for 2-PyH⁻* formation. However, formation by PyH⁺ reduction is likely more kinetically hindered because of the required 1,2-H shift and because PyH⁺ is not favorably adsorbed on the surface. For these reasons, we will focus on the formation path via adsorbed Py reduction when studying the full energetics of 2-PyH⁻* formation.

In a previous study, we investigated the thermodynamics of 2-PyH⁻* formation on the reconstructed GaP(111) surface.[27] We found that the reduction potential for 2-PyH⁻* formation via Py* reduction on GaP(111) (−1.17 V vs. SCE without explicit solvation,[27] −0.97 V vs. SCE with explicit solvation) lies below the CB_min of GaP(111) (−1.58 V vs. SCE at pH 5.2), thus suggesting that the process will be thermodynamically feasible. The thermodynamic driving forces for this process are nearly identical on the GaP(110) and GaP(111) surfaces (0.57 and 0.61 V, respectively). Furthermore, this difference of 0.04 eV is much smaller than the thermodynamic driving force difference observed for other processes on the two surfaces (e.g., 0.36 V for reduction of PyH⁺ to Py* and H*[16]). Thus 2-PyH⁻* formation is

Table 1. Computed reduction potentials (E^0) expressed in V, relative to the saturated calomel electrode (SCE) at pH 5.2 for two classes of reactions: adsorbed pyridine (Py*) reduction reactions that produce adsorbed 2-pyridinyl (2-PyH*), adsorbed deprotonated dihydropyridine (2-PyH⁻*), and adsorbed 1,2-(ortho)-dihydropyridine (o-DHP*); pyridinium (PyH⁺) reduction reactions that produce 1-pyridinyl in solution (1-PyH˙_sol), adsorbed 2-pyridinyl (2-PyH*), adsorbed pyridine (Py*) and adsorbed hydrogen (H*), adsorbed deprotonated dihydropyridine (2-PyH⁻*), and adsorbed 1,2-(ortho)-dihydropyridine (o-DHP*).

Py* reduction reactions[a]	E^0 [V][b]	PyH⁺_sol reduction reactions[a]	E^0 [V][b]
Py*+H⁺_sol+e⁻→2-PyH*	−1.62 (−1.74)[16]	PyH⁺_sol+e⁻→1-PyH˙_sol	−1.44[24]
Py*+H⁺_sol+2e⁻→2-PyH⁻*	−1.09 (−1.41)	PyH⁺_sol+e⁻→2-PyH*	−1.29[17] (−1.31)[16]
Py*+2H⁺_sol+2e⁻→o-DHP*	−0.97 (−1.01)	PyH⁺_sol+e⁻→Py*+H*	−0.91[17] (−0.85)[10]
		PyH⁺_sol+2e⁻→2-PyH⁻*	−0.86 (−1.04)
		PyH⁺_sol+H⁺_sol+2e⁻→o-DHP*	−0.73[17] (−0.79)[17]

[a] * indicates adsorbed species. Subscript "sol" indicates species in solution. [b] E^0 values for heterogeneous reduction pathways were computed by using our mixed implicit–explicit solvation approach for the cluster surface; E^0 values obtained with only implicit solvation are given in parentheses. Refs. [10], [16], [17], and [24] provide the data as indicated; the rest are from this work.

less likely to explain the observed difference in activity between the two surfaces if this is the rate-controlling step in the reaction. However, the adsorption energy of Py on GaP(110) is more favorable than on GaP(111), which could lead to a higher concentration of active Py* sites on GaP(110) compared to GaP(111).[16] This change in site density in turn could be responsible for the higher observed activity of GaP(110), if the complete single-site reaction energetics over the two surfaces is comparable.

Next, by comparing the reduction potentials reported in Table 1, we determine whether 2-PyH⁻* formation can compete with formation of other previously proposed intermediates and other PyH⁺ reduction pathways previously identified. We predict that the reduction potentials for 2-PyH⁻* formation are much less negative than the reduction potentials for formation of adsorbed 2-pyridinyl radical (2-PyH·*)—a catalytic intermediate that we recently considered[16]—by 0.53 and 0.43 V for formation through adsorbed Py reduction and PyH⁺ reduction, respectively. This is an expected result, given the closed-shell nature of 2-PyH⁻ and the radical nature of 2-PyH·. A comparison of the reduction potentials reported in Table 1 also suggests that formation of o-DHP* remains the most thermodynamically favorable step and that o-DHP* is more likely to be the dominant catalytic species in this system. However, although the reduction potentials for 2-PyH·* formation are significantly more negative than those for o-DHP* formation (by 0.65 and 0.56 V for formation through Py* reduction and PyH⁺ reduction, respectively), the reduction potentials for 2-PyH⁻* and o-DHP* formation are quite similar (differing by only 0.12 and 0.13 V for formation through Py* reduction and PyH⁺ reduction, respectively). These results suggest that 2-PyH⁻* formation might be able to compete with o-DHP* formation. Furthermore, 2-PyH⁻* formation might be kinetically favored, as it requires the transfer of fewer protons and electrons. We investigate this hypothesis at the end of the Results section below. On the other hand, the relatively large pK_a calculated for o-DHP* (13.4) in our previous study[13] suggests that 2-PyH⁻* might become protonated once formed, resulting in o-DHP* formation. Ultimately, assessing the kinetics of protonation and the attendant lifetime of 2-PyH⁻* will be key to determining whether this species is involved in the catalysis. This aspect is the subject of an ongoing investigation in our group.

Reaction of adsorbed deprotonated dihydropyridine and adsorbed dihydropyridine with CO_2

We now consider the energetics of CO_2 reduction to HCOO⁻ by hydride transfer from 2-PyH⁻* to establish whether the latter can effectively catalyze this reaction. Furthermore, given that o-DHP* formation is expected to compete with 2-PyH⁻* formation, here we also present the energetics for CO_2 reduction to HCOO⁻ by hydride transfer from o-DHP* and compare these predictions. ΔG and $\Delta G^{\ddagger}$ values at room temperature computed by using our mixed implicit–explicit solvation approach for these two reactions are given in Table 2. The struc-

Table 2. Computed reaction free energies (ΔG) and activation free energies ($\Delta G^{\ddagger}$) at 298.15 K for reaction of adsorbed deprotonated dihydropyridine (2-PyH⁻*) and adsorbed 1,2-(ortho)-dihydropyridine (o-DHP*) with CO_2 to form HCOO⁻.

Reaction[a]	ΔG [kcal mol⁻¹][b]	$\Delta G^{\ddagger}$ [kcal mol⁻¹][b]
2-PyH⁻* + $CO_{2,sol}$ → Py* + HCOO⁻$_{sol}$	−26.9	+7.6
o-DHP* + $CO_{2,sol}$ → PyH⁺$_{sol}$ + HCOO⁻$_{sol}$	−10.2	+25.2

[a] * indicates adsorbed species. Subscript "sol" indicates species in solution. [b] ΔG and $\Delta G^{\ddagger}$ were computed by using the GaP(110) cluster model solvated with our mixed implicit–explicit approach, as described in the Theoretical Methods section.

tures used to calculate the energetics for hydride transfer from 2-PyH⁻* to CO_2 and from adsorbed o-DHP to CO_2 are displayed in Figure 1 and Figure 2, respectively.

We predict that CO_2 reduction to HCOO⁻ by hydride transfer from 2-PyH⁻* is both thermodynamically and kinetically more favorable than CO_2 reduction to HCOO⁻ by hydride transfer from o-DHP*. These findings are not surprising, given that 2-PyH⁻ is a negatively charged species equivalent to deprotonated o-DHP and thus will have a much larger driving force to transfer a hydride to CO_2. Our computed ΔG and $\Delta G^{\ddagger}$ values therefore confirm what we already predicted in our previous report based on our calculated thermodynamic hydricities:[17] 2-PyH⁻* is a much better catalytic intermediate for CO_2 reduction by hydride transfer than o-DHP*. Indeed, the large free energy barrier predicted for hydride transfer from o-DHP* suggests that it is unlikely to be an active hydride shuttle under
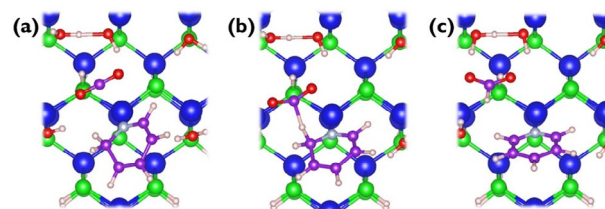

Figure 1. Top view of the (a) initial state, (b) transition state, and (c) final state used to calculate the energetics for the reaction of adsorbed deprotonated dihydropyridine (2-PyH⁻*) with CO_2 to form adsorbed pyridine (Py) and HCOO⁻ on the GaP(110) cluster model solvated with our mixed implicit–explicit approach. Ga atoms are represented in blue, P atoms in green, C atoms in purple, N atoms in light blue, O atoms in red, and H atoms in off-white.
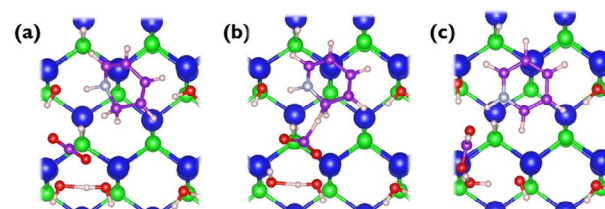

Figure 2. Top view of the (a) initial state, (b) transition state, and (c) final state used to calculate the energetics for the reaction of adsorbed 1,2-(ortho)-dihydropyridine (o-DHP*) with CO_2 to form pyridinium (PyH⁺) and HCOO⁻ on the GaP(110) cluster model solvated with our mixed implicit–explicit approach. The color scheme is the same as in Figure 1.

the room temperature conditions at which the experiments are conducted.

Full energetics of adsorbed deprotonated dihydropyridine formation on GaP(110)

Having confirmed that 2-PyH$^-$* formation is thermodynamically favored on GaP(110) and that 2-PyH$^-$* is a better catalyst for CO_2 reduction than o-DHP*, we now determine whether the formation of 2-PyH$^-$* is kinetically feasible. We recently investigated the full energetics of 2-PyH$^-$* formation by surface hydride transfer to Py* and found that this process is kinetically hindered.[17] Here, we characterize the full energetics of 2-PyH$^-$* formation via a different mechanism: transfer of two photoexcited electrons from the surface and a proton from solution to Py*. We do not study the energetics of 2-PyH$^-$* formation by a two-electron reduction of solvated PyH$^+$, as we previously established that PyH$^+$ is not favorably adsorbed on GaP(110).[10,11,13] Thus, we expect PyH$^+$ reduction to an adsorbed species (e.g., 2-PyH$^-$*) to be more kinetically hindered than Py* reduction coupled with a proton transfer from solution.
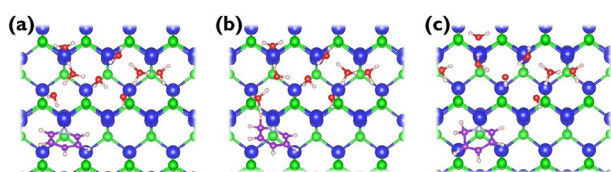

Figure 3. Top view of the (a) initial state, (b) transition state, and (c) final state used to calculate the energetics of adsorbed deprotonated dihydropyridine (2-PyH$^-$*) formation by transfer of two photoexcited electrons and a proton from solution to adsorbed pyridine (Py*). The color scheme is the same as in Figure 1.

The structures used to calculate the energetics of the reaction are illustrated in Figure 3. The proton in solution and the two electrons in the surface were simulated by using an approach introduced by Nørskov and co-workers.[51] In this approach, the reactant structure is formed by adding an extra hydrogen atom in the explicit water layer modeled on top of a solid surface used to simulate the electrode surface. The hydrogen atom then spontaneously separates into a proton that remains solvated by the explicit water molecules on top of the surface and an electron that goes into the surface. PBCs are required to describe properly the distribution of excess electron density in the surface model. In this case, we added two hydrogen atoms because we needed two electrons localized in the surface to simulate the reaction under study. It is crucial to include enough explicit water molecules arranged so that the newly formed protons are stabilized by hydrogen bonds. This will ensure that each neutral hydrogen atom will separate into an electron that goes to the surface and a proton that attaches itself to a water molecule to form hydronium, H_3O^+. In this study, each hydronium ion was solvated by three explicit water molecules so that stable Eigen cations ($H_9O_4^+$) were formed

upon transfer of the electrons to the surface. We verified that the hydrogen atoms separated into solvated protons (i.e., Eigen cations) on top of the surface and electrons in the surface by analyzing the Bader charges[52,53] in the reactant structure (Figure 3a). We found that the total Bader charge of the atoms belonging to the slab was $-1.00\,e$, which qualitatively suggests that the desired electron transfer has occurred. Note that the difference in the surface total Bader charge between the reactant and product is $1.64\,e$ (i.e., approximately $0.82\,e$ per electron transferred away from the surface in the reaction under study), which is comparable to the differences reported by Chan and Nørskov (ca. $0.84\,e$ per electron) for a Heyrovsky proton–electron transfer step in which one electron is transferred from the surface to a proton in solution.[54] Having established that we obtained the desired separation of the added hydrogen atoms into electrons and protons, we decided not to introduce additional water molecules, to facilitate the convergence of the NEB calculation and limit its computational cost.

Two electrons are transferred out of the GaP(110) surface during the course of the 2-PyH$^-$* formation reaction. This leads to a significant increase in the work function (Φ) of the surface as the reaction proceeds, because it becomes less favorable to remove electrons from the surface once the "additional" electrons are removed. The density of states analysis for reactant, transition state, and product (see the Supporting Information) confirms this expected shift in work function, as it shows a shift of the Fermi level upon transfer of the two electrons away from the surface for both the GaP(110) and the reconstructed GaP(111) surfaces (Figures S1 and S2). The simulation thus represents a system at constant charge as opposed to a system at constant potential. By contrast, in the experiment, the semiconductor surface is continuously illuminated at constant potential.[1] For this reason, an appropriate model of the system should replenish photoexcited electrons in the surface as they are removed (i.e., the model should capture the constant potential nature of the experiment). To accomplish this, we employed a methodology recently developed by Chan and Nørskov[54,55] to determine ΔG and $\Delta G^\ddagger$ values at constant potential (i.e., at constant Φ). This method uses the computed Bader charge and Φ differences to extrapolate to the infinite-cell limit, in which Φ remains constant at the Φ of either the reactant structure ($\Phi_{Reactant}$) or of the product structure ($\Phi_{Product}$). These two data points establish the dependence of the reaction energy on Φ in general, thus allowing the reaction energy to be computed at any Φ. The same approach can be applied to compute potential-dependent $\Delta G^\ddagger$ values, where the free energy, Bader charge, and Φ of the product structure are replaced with those of the transition-state structure. Surface Bader charges, Φ values, and extrapolated ΔG and $\Delta G^\ddagger$ values calculated in this study are summarized in Table 3. More details on how these quantities were computed are provided in the Supporting Information. The relevant ΔG and $\Delta G^\ddagger$ values in this work are computed at $\Phi_{CBM} = -CB_{min}$ GaP(110), as this represents the energy of photoexcited electrons when the system is under constant illumination. By using this approach, we predict that this hypothesized reaction has a

Table 3. Surface Bader charge (q), work function (Φ), and extrapolated free energy differences at room temperature (ΔG_{298K}) for the formation of adsorbed deprotonated dihydropyridine (2-PyH$^-$*) on the GaP(110) surface.

Geometry	q [e][a]	Φ [kcal mol^{-1}]	ΔG_{298K} [kcal mol^{-1}][b]		
			at $\Phi = \Phi_{Reactant}$	at $\Phi = \Phi_{Product}$ or $\Phi = \Phi_{TS}$	at $\Phi = \Phi_{CBM}$
Reactant (Py* + 2e$^-$ + H$^+$)	−1.00	63.7	–	–	–
TS (Py* + 2e$^-$ + H$^+$ → 2-PyH$^-$*)	−0.39	77.3	12.0	20.3	13.6
Product (2-PyH$^-$*)	0.64	83.5	−47.9	−15.4	−43.7

[a] Negative surface charge indicates excess electrons. [b] ΔG_{298K} columns represent activation free energies ($\Delta G^{\ddagger}$) in the transition-state (TS) row and reaction free energies (ΔG) in the Product row.
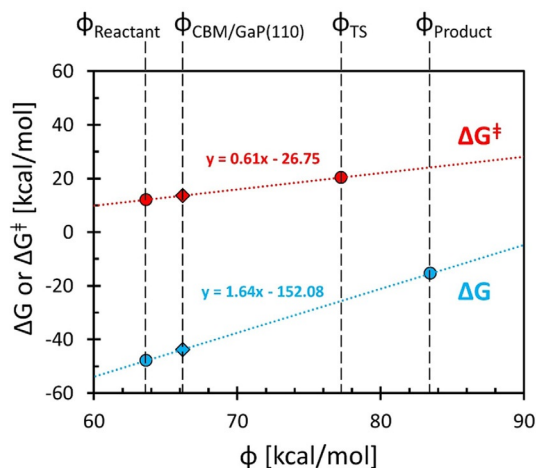

Figure 4. Potential-dependent reaction free energy (ΔG) and activation free energy ($\Delta G^{\ddagger}$) for the formation of adsorbed deprotonated dihydropyridine (2-PyH$^-$*) via Py* + 2e$^-$ + H$^+$ → 2-PyH$^-$* over the GaP(110) surface. Circles represent data computed directly from density functional theory (DFT)-derived free energies, work functions (Φ), and Bader charges calculated in this work. The diamonds represent data that are interpolated to the GaP(110) conduction band minimum (CB$_{min}$) computed in a previous study.[16]

moderate $\Delta G^{\ddagger}$ value of 13.6 kcal mol^{-1} at Φ_{CBM} and a large thermodynamic driving force with a ΔG of −43.7 kcal mol^{-1} at Φ_{CBM} (Figure 4). Overall, based on the computed full energetics of this reaction, we expect 2-PyH$^-$* formation to be feasible on the GaP(110) surface under illumination. Qualitatively similar results were obtained for the reconstructed GaP(111) surface (Figure S4 and Table S2).

Summary and Conclusions

We investigated the viability of a newly proposed hydrogenated N-heterocycle catalytic intermediate for Py-catalyzed CO$_2$ reduction at the GaP(110) surface. This intermediate, 2-PyH$^-$*, was identified recently as a better hydride donor for CO$_2$ reduction than the previously proposed o-DHP* catalytic intermediate.[17] Furthermore, in a separate study, we predicted that formation of this species is thermodynamically viable on the illuminated, reconstructed GaP(111), CdTe(111), and CuInS$_2$(112) surfaces.[27] Herein, we predicted that 2-PyH$^-$ is favorably adsorbed on GaP(110) at room temperature, thus suggesting that this species is a plausible candidate for an adsorbed co-

catalyst. Furthermore, the computed reduction potentials for 2-PyH$^-$* formation show that this species can form on the GaP(110) surface by transfer of photoexcited electrons and that this process might be able to compete with the formation of o-DHP*. However, o-DHP* formation remains the most thermodynamically favored step and might occur through protonation of 2-PyH$^-$* based on the previously computed pK$_a$ of o-DHP*.[13] This aspect is currently under investigation in our group. Based on these results, we computed and compared the reaction energetics for CO$_2$ reduction to HCOO$^-$ by hydride transfer from 2-PyH$^-$* versus o-DHP*. We found that CO$_2$ reduction by hydride transfer from 2-PyH$^-$* is favored from both kinetic and thermodynamic points of view. This finding confirms our prediction based on our computed thermodynamic hydricities that 2-PyH$^-$*,[17] if formed and with a long-enough lifetime before being protonated, would be a better catalyst than o-DHP* for CO$_2$ reduction by hydride transfer. Finally, we investigated the full energetics of 2-PyH$^-$* formation by transfer of two photoexcited electrons and a proton from solution to Py* and found that this process is kinetically feasible on the GaP(110) surface under illumination. Overall, based on the results presented herein, we conclude that 2-PyH$^-$* is a valid candidate as an active co-catalyst for CO$_2$ reduction on p-GaP photoelectrodes, acting as a viable hydride shuttle to CO$_2$.

Conflict of interest

The authors declare no conflict of interest.

[1] E. E. Barton, D. M. Rampulla, A. B. Bocarsly, *J. Am. Chem. Soc.* **2008**, *130*, 6342–6344.

[2] C. Lin, G. Seshadri, A. B. Bocarsly, *J. Electroanal. Chem.* **1994**, *372*, 145–150.

[3] E. Barton Cole, P. S. Lakkaraju, D. M. Rampulla, A. J. Morris, E. Abelev, A. B. Bocarsly, *J. Am. Chem. Soc.* **2010**, *132*, 11539–11551.

[4] J. H. Jeon, P. M. Mareeswaran, C. H. Choi, S. I. Woo, *RSC Adv.* **2014**, *4*, 3016–3019.

[5] J. Yuan, C. Hao, *Sol. Energy Mater. Sol. Cells* **2013**, *108*, 170–174.

[6] J. Yuan, L. Zheng, C. Hao, *RSC Adv.* **2014**, *4*, 39435–39438.

[7] J. A. Keith, E. A. Carter, *Chem. Sci.* **2013**, *4*, 1490–1496.

[8] J. A. Keith, E. A. Carter, *J. Phys. Chem. Lett.* **2013**, *4*, 4058–4063.

[9] Corrigendum: J. A. Keith, E. A. Carter, *J. Phys. Chem. Lett.* **2015**, *6*, 568.

[10] M. Lessio, E. A. Carter, *J. Am. Chem. Soc.* **2015**, *137*, 13248–13251.

[11] J. A. Keith, A. B. Muñoz-García, M. Lessio, E. A. Carter, *Top. Catal.* **2015**, *58*, 46–56.

[12] C. X. Kronawitter, M. Lessio, P. Zahl, A. B. Muñoz-García, P. Sutter, E. A. Carter, B. E. Koel, *J. Phys. Chem. C* **2015**, *119*, 28917–28924.

[13] M. Lessio, C. Riplinger, E. A. Carter, *Phys. Chem. Chem. Phys.* **2016**, *18*, 26434–26443.

[14] A. B. Muñoz-García, E. A. Carter, *J. Am. Chem. Soc.* **2012**, *134*, 13600–13603.

[15] C. X. Kronawitter, M. Lessio, P. Zhao, C. Riplinger, A. Boscoboinik, D. E. Starr, P. Sutter, E. A. Carter, B. E. Koel, *J. Phys. Chem. C* **2015**, *119*, 17762–17772.

[16] M. Lessio, T. P. Senftle, E. A. Carter, *ACS Energy Lett.* **2016**, *1*, 464–468.

[17] M. Lessio, J. M. Dieterich, E. A. Carter, *J. Phys. Chem. C* **2017**, *121*, 17321–17331.

[18] K. Hayashi, M. Ashizuka, R. C. Bradt, H. Hirano, *Mater. Lett.* **1982**, *1*, 116–118.

[19] Y. Hu, *Solar Fuel Generation on Semiconductors: Photo-Assisted H_2 Evolution on a Novel Delafossite $AgRhO_2$ and a P-GaP (111) Surface With {110} Faces Revealed by Etching for CO_2 Reduction* (Doctoral Thesis), Princeton University, **2015**.

[20] C. X. Kronawitter, Z. Chen, P. Zhao, X. Yang, B. E. Koel, *Catal. Sci. Technol.* **2017**, *7*, 831–837.

[21] P. K. Giesbrecht, D. E. Herbert, *ACS Energy Lett.* **2017**, *2*, 549–555.

[22] C.-H. Lim, A. M. Holder, J. T. Hynes, C. B. Musgrave, *J. Am. Chem. Soc.* **2014**, *136*, 16081–16095.

[23] J. A. Tossell, *Comput. Theor. Chem.* **2011**, *977*, 123–127.

[24] J. A. Keith, E. A. Carter, *J. Am. Chem. Soc.* **2012**, *134*, 7580–7583.

[25] C.-H. Lim, A. M. Holder, C. B. Musgrave, *J. Am. Chem. Soc.* **2013**, *135*, 142–154.

[26] M. Z. Ertem, S. J. Konezny, C. M. Araujo, V. S. Batista, *J. Phys. Chem. Lett.* **2013**, *4*, 745–748.

[27] T. P. Senftle, M. Lessio, E. A. Carter, *ACS Cent. Sci.* **2017**, *3*, 968–974.

[28] W. Kohn, L. J. Sham, *Phys. Rev.* **1965**, *140*, A1133.

[29] F. Neese, *Wiley Interdiscip. Rev. Comput. Mol. Sci.* **2012**, *2*, 73–78.

[30] A. D. Becke, *Phys. Rev. A* **1988**, *38*, 3098.

[31] C. Lee, W. Yang, R. G. Parr, *Phys. Rev. B* **1988**, *37*, 785–789.

[32] A. D. Becke, *J. Chem. Phys.* **1993**, *98*, 5648–5652.

[33] A. Bergner, M. Dolg, W. Küchle, H. Stoll, H. Preuß, *Mol. Phys.* **1993**, *80*, 1431–1441.

[34] T. Leininger, A. Berning, A. Nicklass, H. Stoll, H.-J. Werner, H.-J. Flad, *Chem. Phys.* **1997**, *217*, 19–27.

[35] P. C. Hariharan, J. A. Pople, *Theor. Chim. Acta* **1973**, *28*, 213–222.

[36] M. M. Francl, W. J. Pietro, W. J. Hehre, J. S. Binkley, M. S. Gordon, D. J. De-Frees, J. A. Pople, *J. Chem. Phys.* **1982**, *77*, 3654–3665.

[37] T. H. Dunning, *J. Chem. Phys.* **1989**, *90*, 1007–1023.

[38] S. Grimme, *J. Comput. Chem.* **2006**, *27*, 1787–1799.

[39] A. V. Marenich, C. J. Cramer, D. G. Truhlar, *J. Phys. Chem. B* **2009**, *113*, 6378–6396.

[40] A. A. Isse, A. Gennaro, *J. Phys. Chem. B* **2010**, *114*, 7894–7899.

[41] J. A. Keith, E. A. Carter, *J. Chem. Theory Comput.* **2012**, *8*, 3187–3206.

[42] J. Baker, *J. Comput. Chem.* **1986**, *7*, 385–395.

[43] G. Kresse, J. Furthmüller, *Comput. Mater. Sci.* **1996**, *6*, 15–50.

[44] G. Kresse, J. Furthmüller, *Phys. Rev. B* **1996**, *54*, 11169–11186.

[45] G. Kresse, J. Hafner, *Phys. Rev. B* **1993**, *48*, 13115–13118.

[46] J. P. Perdew, M. Ernzerhof, K. Burke, *Phys. Rev. Lett.* **1996**, *77*, 3865–3868.

[47] P. E. Blöchl, *Phys. Rev. B* **1994**, *50*, 17953–17979.

[48] G. Kresse, D. Joubert, *Phys. Rev. B* **1999**, *59*, 1758–1775.

[49] H. J. Monkhorst, J. D. Pack, *Phys. Rev. B* **1976**, *13*, 5188.

[50] G. Henkelman, B. P. Uberuaga, H. Jónsson, *J. Chem. Phys.* **2000**, *113*, 9901–9904.

[51] J. Rossmeisl, E. Skúlason, M. E. Björketun, V. Tripkovic, J. K. Nørskov, *Chem. Phys. Lett.* **2008**, *466*, 68–71.

[52] R. F. W. Bader, *Atoms in Molecules: A Quantum Theory*, Oxford University Press, New York, **1990**.

[53] W. Tang, E. Sanville, G. Henkelman, *J. Phys. Condens. Matter* **2009**, *21*, 084204.

[54] K. Chan, J. K. Nørskov, *J. Phys. Chem. Lett.* **2015**, *6*, 2663–2668.

[55] K. Chan, J. K. Nørskov, *J. Phys. Chem. Lett.* **2016**, *7*, 1686–1690.